

Detailed investigation of the analysis conditions in the evaluation of bonded joints by cohesive zone models

R.J.B. Rocha^a, R.D.S.G. Campilho^{a,b,*}

^a Departamento de Engenharia Mecânica, Instituto Superior de Engenharia do Porto, Instituto Politécnico do Porto, Rua Dr. António Bernardino de Almeida, 431, 4200-072 Porto, Portugal

^b INEGI – Pólo FEUP, Rua Dr. Roberto Frias, s/n, 4200-465 Porto, Portugal

* raulcampilho@gmail.com

Abstract. Cohesive Zone Models (CZM) are widely used for the strength prediction of adhesive joints. This work studies the influence of different conditions used in CZM simulations to model a thin adhesive layer in single-lap joints (SLJ) under a tensile loading, for an estimation of their influence on the strength prediction under diverse geometrical and material conditions. Adhesives ranging from brittle to highly ductile and overlap lengths (L_0) between 12.5 and 50 mm were considered. Several damage initiation and growth criteria were tested. The analysis carried out in this work allowed to conclude that CZM is a powerful technique for strength prediction of bonded joints, provided that the modelling conditions are properly defined.

1. Introduction

Adhesive technology has earned interest in the major fields of industrial applications, since adhesively-bonded joints have many advantages over conventional mechanical fasteners. Among other benefits, this joining method preserves the integrity of parent materials, gives the possibility of join different materials and provides more uniform stress distributions. Adhesive bonds also promote good strength-weight and cost-effectiveness ratios. On the other hand, limitations of bonded joints include the disassembly difficulty without causing damage, low resistance to temperature and humidity, the requirement of a surface treatment and joint design orientated towards the elimination of peel stresses [1]. The strength prediction of bonded joints began with analytical techniques, firstly performed by Volkersen [2]. With these techniques, bonded joints are quickly analysed, although with simplifying assumptions regarding the material behaviour (e.g. neglecting the adhesives' plasticity), loading and boundary conditions. Numerical techniques (i.e. finite elements (FE)) are more adequate. Barenblatt [3] and Dugdale [4] proposed the concept of cohesive zone to describe damage under static loads with no need of an initial crack. Since then, CZM were improved and tested to simulate crack initiation and growth. CZM are based on cohesive elements [5], connecting solid elements of structures and can be easily implemented in FE software to model the fracture behaviour. This method simulates damage along a predefined crack path by the establishment of traction-separation laws that correlate the cohesive tractions (t_n for tension and t_s for shear) with the relative displacements (δ_n for tension and δ_s for shear). Different criteria can be used to assess damage initiation and growth. Gustafson and Waas [6] have investigated the influence of the constitutive parameters of the adhesive for the CZM analysis of several tests commonly used to describe the joints' performance. The Double-Cantilever Beam (DCB), the End-Notched Flexure (ENF) test and the SLJ were evaluated. It was found that the DCB test is only sensitive to the fracture toughness in tension (G_{IC}), which makes this test suitable to define this parameter for



CZM simulations. Oppositely, the ENF and SLJ results are influenced by several parameters, such as G_{IC} , fracture toughness in shear (G_{IIC}) and the shear cohesive strength (t_s^0). The tensile cohesive strength (t_n^0) promotes a negligible effect in the studied tests and, thus, it can be estimated independently to those tests. CZM is a precise technique for bonded joints, provided that the modelling conditions are those known to work well for this type of structures (for example using a quadratic stress criterion for damage initiation and a linear power law energetic criterion for damage propagation).

This work evaluates the influence of the different damage initiation and growth criteria on the P_m estimation for SLJ, considering different geometrical and material conditions. Validation with experimental data is considered. Adhesives ranging from brittle to highly ductile and L_O between 12.5 and 50 mm were considered.

2. Experimental work

The high strength and ductile aluminium alloy AA6082 T651 was chosen for the adherends. The tensile mechanical properties of this material were obtained in the work of Campilho et al. [7]: Young's modulus (E) of 70.07 ± 0.83 GPa, tensile yield stress (σ_y) of 261.67 ± 7.65 MPa, tensile strength (σ_f) of 324 ± 0.16 MPa and tensile failure strain (ε_f) of $21.70 \pm 4.24\%$. Three structural adhesives were tested: the brittle epoxy Araldite® AV138, the ductile epoxy Araldite® 2015 and the ductile polyurethane Sikaforce® (Sika®, Baar, Switzerland) 7752, characterized in previous works regarding the most relevant properties [7-9]. The tensile mechanical properties (E , σ_y , σ_f and ε_f) were obtained by bulk tests on specimens with dogbone shape (NF 76-142 standard). The shear mechanical properties estimated with Thick Adherend Shear Tests (TAST) considering the ISO 11003-2 standard. The G_{IC} and G_{IIC} were taken from DCB and ENF tests, respectively, using beam theories. The DCB tests were carried out according to the ISO 15024-1 standard. No standard is available for ENF tests; thus, common practices for composite toughness determination were followed. The properties of the adhesives are detailed in Table 1.

Table 1 – Properties of the adhesives Araldite® AV138, Araldite® 2015 and Sikaforce® 7752 [7-9].

Property	AV138	2015	7752
Young's modulus, E [GPa]	4.89 ± 0.81	1.85 ± 0.21	0.49 ± 0.09
Poisson's ratio, ν	0.35 ^a	0.33 ^a	0.30 ^a
Tensile yield stress, σ_y [MPa]	36.49 ± 2.47	12.63 ± 0.61	3.24 ± 0.48
Tensile strength, σ_f [MPa]	39.45 ± 3.18	21.63 ± 1.61	11.48 ± 0.25
Tensile failure strain, ε_f [%]	1.21 ± 0.10	4.77 ± 0.15	19.18 ± 1.40
Shear modulus, G [GPa]	1.56 ± 0.01	0.56 ± 0.21	0.19 ± 0.01
Shear yield stress, τ_y [MPa]	25.1 ± 0.33	14.6 ± 1.3	5.16 ± 1.14
Shear strength, τ_f [MPa]	30.2 ± 0.40	17.9 ± 1.8	10.17 ± 0.64
Shear failure strain, γ_f [%]	7.8 ± 0.7	43.9 ± 3.4	54.82 ± 6.38
Toughness in tension, G_{IC} [N/mm]	0.20 ^b	0.43 ± 0.02	2.36 ± 0.17
Toughness in shear, G_{IIC} [N/mm]	0.38 ^b	4.70 ± 0.34	5.41 ± 0.47

^a manufacturer's data

^b estimated in reference [7]

The SLJ geometry and characteristic dimensions are presented in Figure 1. The tested geometrical parameter in this work is L_O . The dimensions of the specimens are: joint length between grips $L_T=170$ mm, adherends' thickness $t_p=3$ mm, width $B=25$ mm, adhesive thickness $t_A=0.2$ mm and $L_O=12.5, 25, 37.5$ and 50 mm. Joint preparation before bonding consisted of sandblasting and cleaning with acetone, which resulted in full cohesive failures of the adhesive layer in all specimens. Assembly was undertaken in a steel mould and calibrated nylon wire was placed between the adherends to produce the desired value of t_A . Curing was carried out at room temperature for one week. In order to perform the experimental tests at room temperature, a Shimadzu® (Shimadzu, Kyoto, Japan) AG-X 100 testing machine with a 100 kN load cell was used. The displacement rate was 1 mm/min. Five samples were considered for each joint configuration.

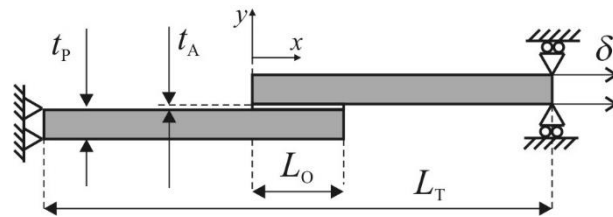


Figure 1 – Geometry and characteristic dimensions of the SLJ specimens [8]

3. Numerical work

The software ABAQUS® (Dassault Systèmes, Vélizy-Villacoublay, France) was used for P_m prediction by CZM. The adherends were modelled as elastic-plastic isotropic materials, and by 4-node plane-strain elements (CPE4 from ABAQUS®). The adhesive layer was modelled by 4-node cohesive elements. Both simulations consisted of a two-dimensional (2D) and geometrically non-linear analysis. In order to reduce the computational effort, mesh grading was considered by using the bias effect. CZM are based on a relationship between stresses and relative displacements (in tension or shear) connecting paired nodes of cohesive elements, to simulate the elastic behaviour up to t_n^0 in tension or t_s^0 in shear and subsequent softening up to failure. The areas under the traction-separation laws in tension or shear are equalled to G_{IC} or G_{IIC} , by the respective order. The triangular law assumes an initial linear elastic behaviour followed by linear degradation. Damage initiation can be specified by different criteria, either stress or strain based. The available stress-based damage initiation criteria are the maximum nominal stress (MAXS), quadratic nominal stress (QUADS) and maximum principal stresses (MAXPS) criteria expressed, by the same order, as [10]

$$\max \left\{ \frac{\langle t_n \rangle}{t_n^0}, \frac{t_s}{t_s^0} \right\} = 1 \quad ; \quad \left\{ \frac{\langle t_n \rangle}{t_n^0} \right\}^2 + \left\{ \frac{t_s}{t_s^0} \right\}^2 = 1 \quad ; \quad \left\{ \frac{\langle \sigma_{\max} \rangle}{\sigma_{\max}^0} \right\} = 1. \quad (1)$$

$\langle \rangle$ are the Macaulay brackets, emphasizing that a purely compressive stress state does not initiate damage [11]. σ_{\max} and σ_{\max}^0 represent the current and the allowable maximum principal stress. The strain-based maximum nominal strain (MAXE), quadratic nominal strain criterion (QUADE) and maximum principal strain (MAXPE) criteria are described as (by the same order) [10]

$$\max \left\{ \frac{\langle \varepsilon_n \rangle}{\varepsilon_n^0}, \frac{\varepsilon_s}{\varepsilon_s^0} \right\} = 1 \quad ; \quad \left\{ \frac{\langle \varepsilon_n \rangle}{\varepsilon_n^0} \right\}^2 + \left\{ \frac{\varepsilon_s}{\varepsilon_s^0} \right\}^2 = 1 \quad ; \quad \left\{ \frac{\langle \varepsilon_{\max} \rangle}{\varepsilon_{\max}^0} \right\} = 1, \quad (2)$$

where ε_n and ε_s are the current tensile and shear strain, respectively. ε_n^0 and ε_s^0 are corresponding peak strains. ε_{\max} and ε_{\max}^0 represent the current and the allowable maximum principal strain. By the fulfilment of the above mentioned criteria, the material stiffness initiates a degradation process. Complete separation and failure are predicted by a damage evolution law. The power law criterion states that failure under mixed-mode conditions is governed by a power law interaction of the energies required to cause failure in the individual (normal and shear) modes. It is given by the expression [10]

$$\left\{ \frac{G_I}{G_{IC}} \right\}^\alpha + \left\{ \frac{G_{II}}{G_{IIC}} \right\}^\alpha = 1, \quad (3)$$

where α is the power law parameter, and G_I and G_{II} relate to the work done by the traction and corresponding relative displacements in the normal and shear directions, respectively. The Benzeggagh-Kenane (BK) [12] fracture criterion is particular useful when the critical fracture energies during deformation purely along the first and the second shear directions are the same; i.e., $G_{IIC} = G_{IIIC}$. It is given by

$$G_{IC} + (G_{IIC} + G_{IC}) \left\{ \frac{G_S}{G_T} \right\}^\eta = G_C, \quad (4)$$

where $G_S = G_{II} + G_{III}$, $G_T = G_I + G_S$ and η is a characteristic material parameter. The relevant CZM parameters used in this work were taken from the data of Table 1.

4. Results

4.1. Experimental and numerical joint strength

The average experimental values of P_m and respective deviation for the joints bonded with the three adhesives are depicted in Figure 2. The CZM predictions using the common modelling conditions for bonded joints are also presented (quadratic stress criterion damage initiations and linear power law criterion for growth).

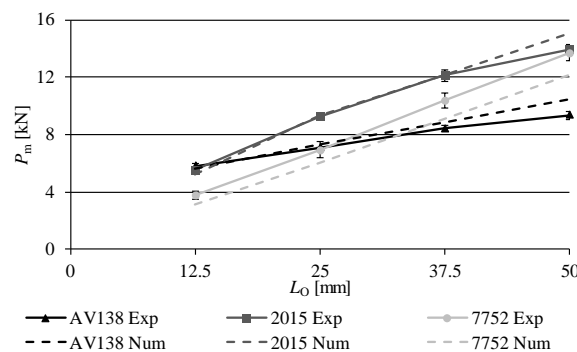


Figure 2 – Experimental and CZM values of P_m for each value of L_0 and adhesive type

Comparing the experimental and numerical results for the adhesive Araldite® AV138 (Figure 2), these were very similar except for $L_0 = 50$ mm, with a maximum relative deviation of 11.8%. Due to the brittleness of the adhesive Araldite® AV138, P_m is attained with minimum plasticization at the overlap edges, justifying the good results obtained with a triangular CZM. A good correlation was found for the joints bonded with the adhesive Araldite® 2015, except for $L_0 = 50$ mm, where P_m was underestimated by 8.0%. Figure 2 presents numerically underestimated values of P_m for all L_0 for the joints bonded with the adhesive Sikaforce® 7752. The under prediction of the P_m values is related to this adhesive's large plasticity, which is not accurately modelled by the triangular CZM.

4.2. Different conditions of the numerical simulations

4.2.1. Damage initiation criterion. First, the stress-based damage initiation criteria were evaluated by comparison between the experimental data, the prediction performed in Section 4.1 (QUADS criterion), and the MAXS and MAXPS criteria. Figure 3 shows the comparative results for the three adhesives. The results for the adhesive Araldite® AV138 (Figure 3 a) show close results to the experimental ones for the MAXS and QUADS criteria, contrarily to MAXPS. Actually, the MAXPS criterion gives identical P_m values irrespectively of L_0 , since failure took place by tensile net failure of the adherends. Between the other two criteria, the QUADS criterion gives more accurate results compared to the experimental data (maximum deviation of 16.9% for the MAXS and 11.8% for the QUADS, both considering $L_0 = 50$ mm). Figure 3 b, related to the Araldite® 2015, presents once more closer results for the MAXS and QUADS criteria. With the MAXPS criterion failure took place by tensile net failure of the adherends. For the presented adhesive, the QUADS criterion gave the closest results to the experiments. The maximum error regarding the experimental data was 8.8% (MAXS), and 8.0% (QUADS) for $L_0 = 50$ mm. The strength prediction performed for the adhesive Sikaforce® 7752 shows that the MAXS and QUADS criteria give P_m under predicted results. The MAXPS criterion revealed, once more, to be a poor choice for P_m . However, evaluation data places the MAXS criterion as the best choice to perform P_m estimation for the joints bonded with this adhesive, since smaller under predictions

were attained for all L_O values. The maximum relative deviations were 17.1% (QUADS), and 15.7% (MAXS), found for $L_O=12.5$ mm.

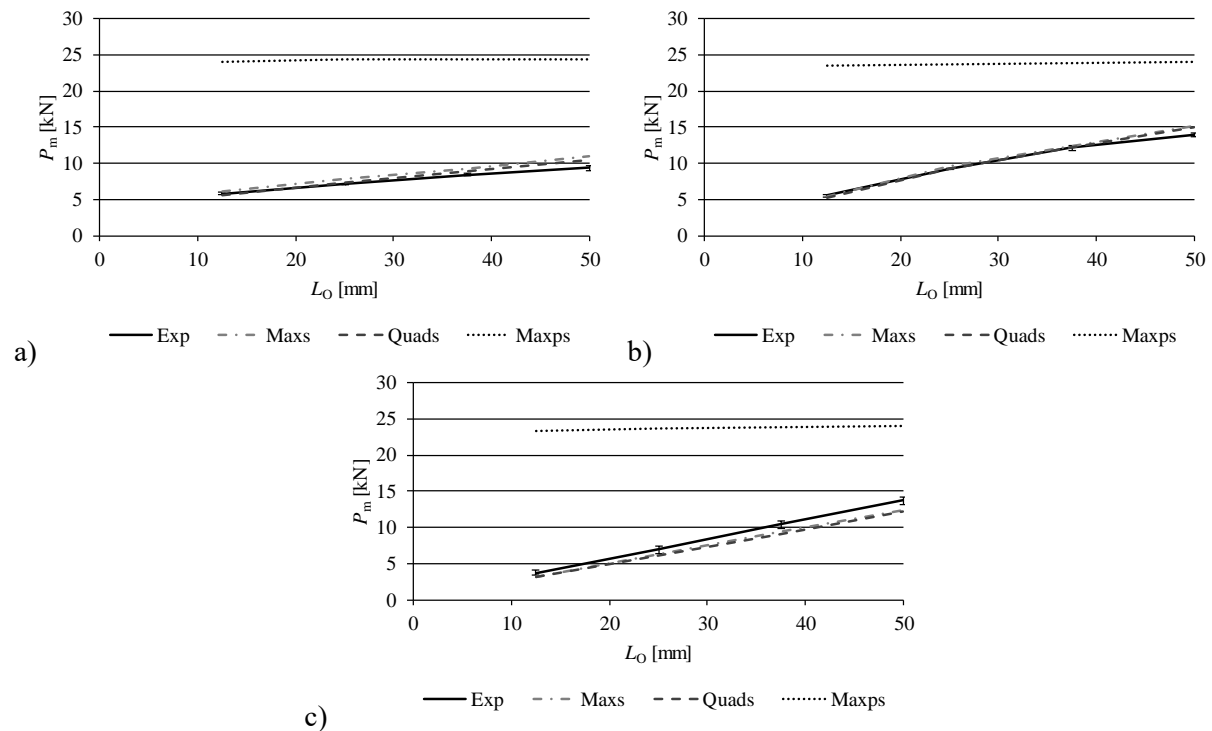


Figure 3 – Comparison between the experimental data and different damage initiation stress criteria for the joints bonded with the adhesive Araldite® AV138 (a), Araldite® 2015 (b) and Sikaforce® 7752 (c)

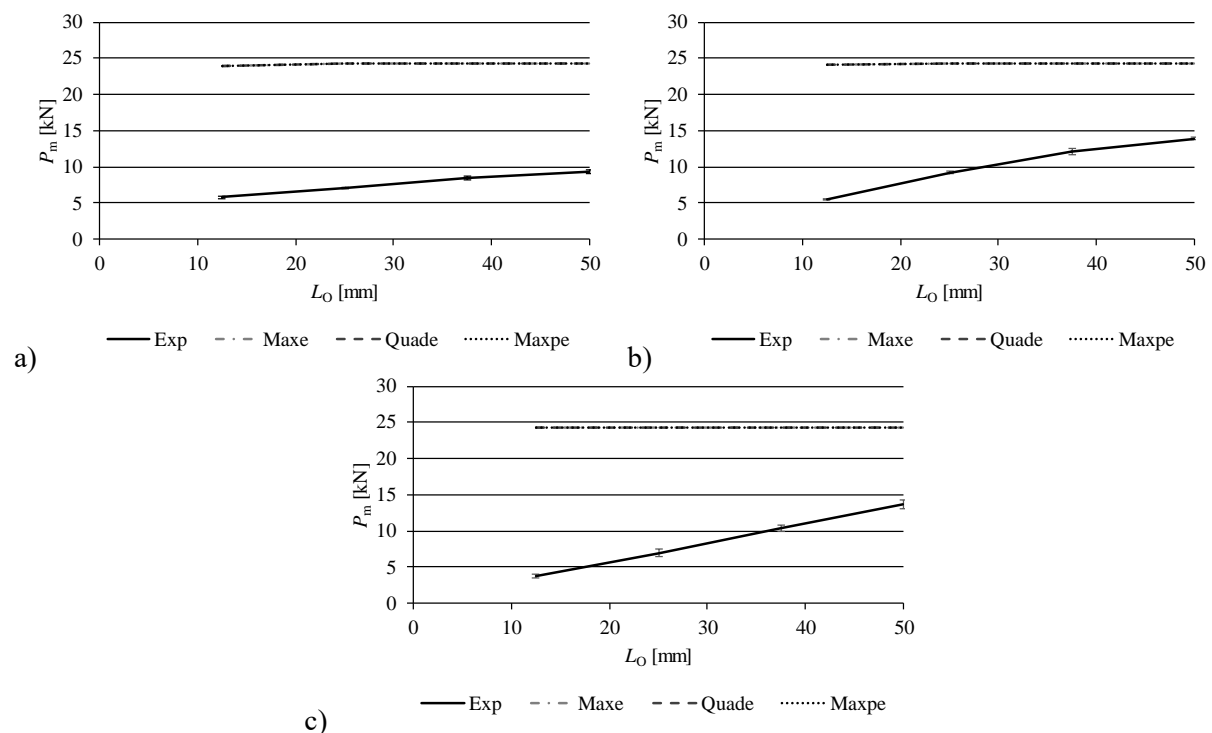


Figure 4 – Comparison between the experimental data and different damage initiation strain criteria for the joints bonded with the adhesive Araldite® AV138 (a), Araldite® 2015 (b) and Sikaforce® 7752 (c)

The evaluation of the strain-based initiation criteria was carried out by comparison between the experimental data, the MAXE, the QUADE and the MAXPE criteria. Figure 4 presents this evaluation for all adhesives. Regardless the adhesive used, strain-based initiation criteria are not suited to simulate damage initiation in the adhesive layer, since they all overshoot by a large amount the experimental results. In some joint configurations, damage initiated at a load close to the tensile net failure load of the adherends. In other configurations, P_m corresponded to the adherends' tensile net failure.

4.2.2. Damage growth criterion. This sub-Section addresses the accuracy of the power law and the BK growth criteria for the P_m prediction of the three adhesives. The power law evaluation was firstly performed by varying the power parameter α (equation (3)), considering values 0.5, 1, 1.5, and 2, for further comparison with the experimental data. The results are presented in Figure 5 for all adhesives.

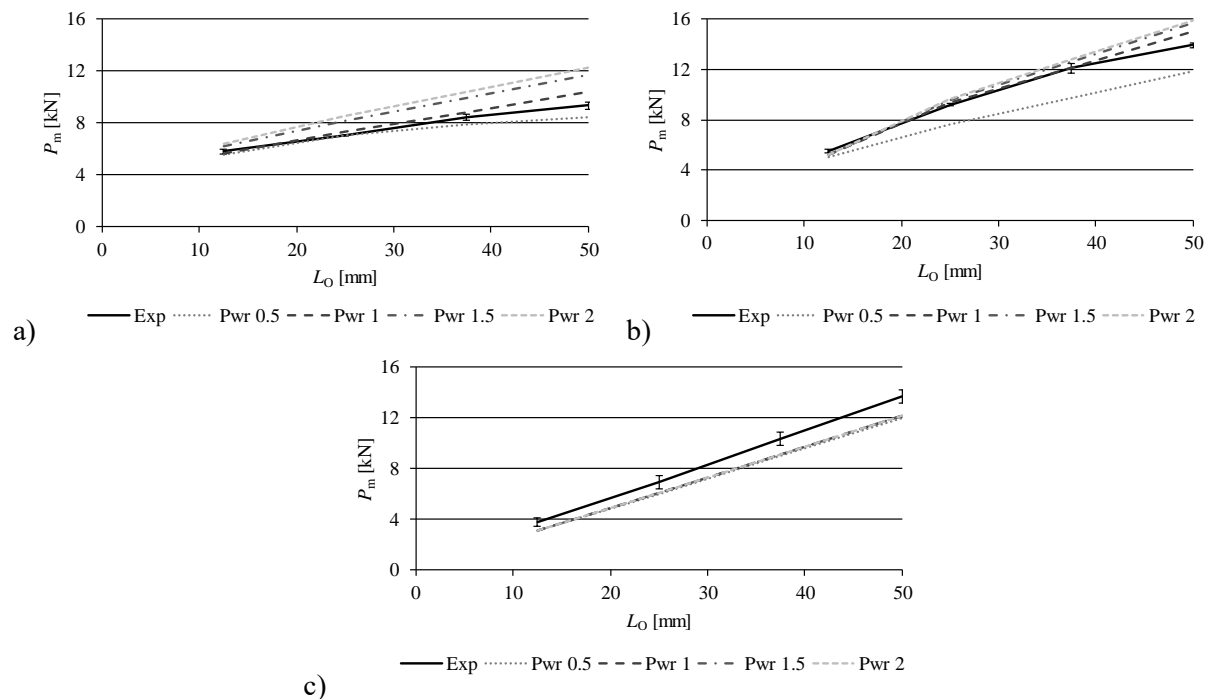


Figure 5 – Comparison between different parameter values of the power law growth criteria for P_m prediction for the joints bonded with the adhesive Araldite® AV138 (a), Araldite® 2015 (b) and Sikaforce® 7752 (c)

Figure 5 a, related to the adhesive Araldite® AV138, reports that the Power 0.5 suits best for this adhesive. Actually, an average deviation of 4.9% was achieved for all L_0 values, followed by Power 1, with an average difference of 5.9%. Power 1.5 over predicts P_m by the average value of 16.2%, while Power 2 gives the worst P_m predictions. As L_0 increases, deviations also grow, regardless the value of the power parameter. The comparison shown in Figure 5 b reveals Power 1 as the best for the joints bonded with the adhesive Araldite® 2015. Power 1.5 and Power 2 predicted P_m with an average deviation of 6.6 and 7.3%, respectively. The Power 0.5 criterion, which was the best choice for the strength prediction of the previous adhesive, presents now the worst P_m estimation. The increase of L_0 promotes the rise of relative deviations, by comparison with the experimental data, equally to what was observed for the Araldite® AV138. The evaluation depicted in Figure 5 c, comparing different parameters of the power law criterion for the adhesive Sikaforce® 7752, provides identical P_m under estimation values, whatsoever were the chosen α or L_0 values.

The evaluation of the BK growth criterion for P_m prediction was performed by comparison with the Power law criterion ($\alpha=1$), and the experimental data. For the characteristic parameter η of equation (4) the values 0.5, 1, and 2.5 were used. It is shown that the condition that provides the most accurate P_m prediction for the adhesive Araldite® AV138 was BK 2.5 (Figure 6 a), with an average deviation of

4.1%, close to that obtained with Power 1 (4.3%). Nonetheless, a more detailed analysis reveals P_m under estimations for the lower L_O values: -7.5, and -1.3% for $L_O=12.5$, and 25 mm, and P_m over estimations for higher L_O values: 0.6, and 7.1% for $L_O=37.5$, and 50 mm, respectively. In Figure 6 b (Araldite® 2015), it is shown that the BK criterion under predicts P_m for the lowest L_O value, by an average error of 4.3% for the three values of η . Oppositely, for higher L_O , big deviations by excess were found: P_m was over predicted by values up to 48.3% ($\eta=0.5$), 47.2% ($\eta=1$), and 16.7% ($\eta=2.5$), attained with $L_O=50$ mm. In view of those deviations, the power law criteria gives the most accurate P_m predictions for this adhesive. The comparison depicted in Figure 6 c, regarding the evaluation of the damage growth criteria for the adhesive Sikaforce® 7752, shows that all criteria underestimate P_m , with very similar average deviations of -17.1, -12.9, -12.2, and -11.3% for $L_O=12.5$, 25, 37.5, and 50 mm, respectively.

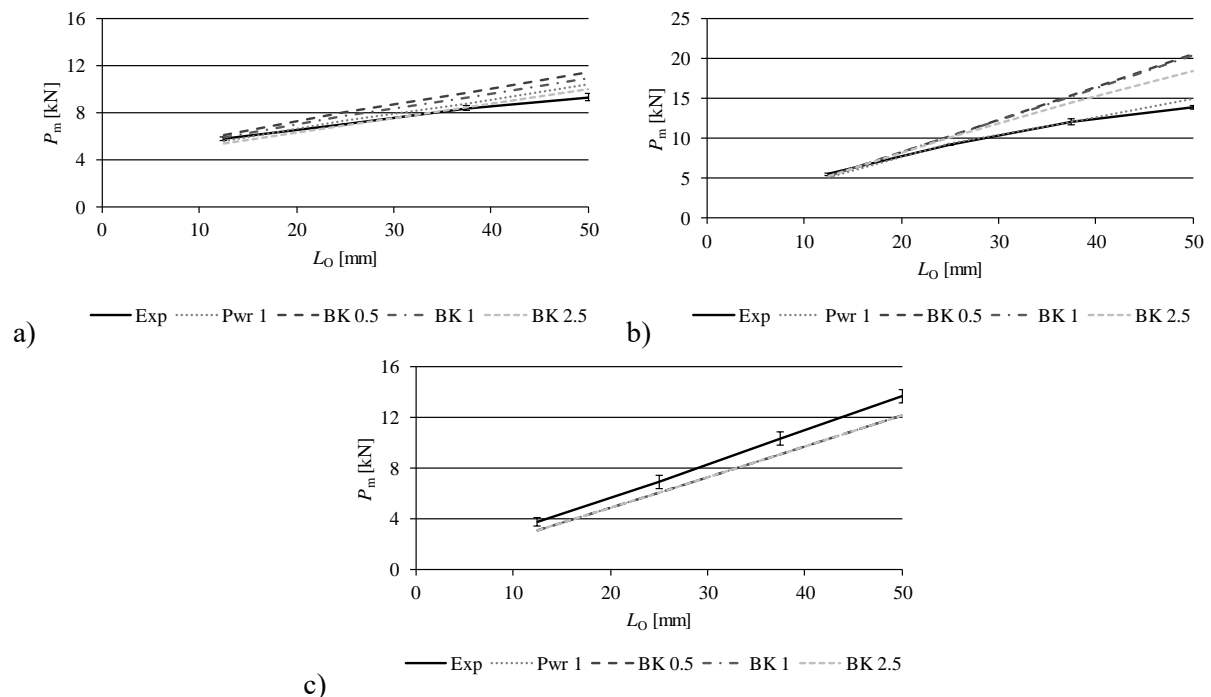


Figure 6 – Comparison between power law and BK growth criteria for P_m prediction for the joints bonded with the adhesive Araldite® AV138 (a), Araldite® 2015 (b) and Sikaforce® 7752 (c)

The evaluation of the BK growth criterion for P_m prediction was performed by comparison with the Power law criterion ($\alpha=1$), and the experimental data. For the characteristic parameter η of equation (4), the values 0.5, 1, and 2.5 were used. It is shown that the condition that provides the most accurate P_m prediction for the adhesive Araldite® AV138 was BK 2.5 (Figure 6 a), with an average deviation of 4.1%, close to that obtained with Power 1 (4.3%). In Figure 6 b (Araldite® 2015), it is shown that the BK criterion under predicts P_m for the lowest L_O value, by an average error of 4.3% for the three values of η . Oppositely, for higher L_O , big deviations by excess were found. The comparison depicted in Figure 6 c, regarding the evaluation of the damage growth criteria for the adhesive Sikaforce® 7752, shows that all criteria underestimate P_m , with very similar average deviations.

5. Conclusions

This work aimed at evaluating different simulation conditions in the CZM analysis for an accurate strength prediction of SLJ. Strength prediction by CZM was performed, using reliable CZM conditions for bonded joints (triangular mixed-mode CZM law, QUADS initiation criterion and linear CZM law). For the adhesives Araldite® AV138 and Araldite® 2015, the P_m prediction was accurate. For the adhesive Sikaforce® 7752, P_m was under predicted by 13.4% (average for all L_O), due to the large plasticity that

this adhesive can endure, which is not correctly modelled by the triangular CZM. After this study, different modelling conditions were tested, whose main conclusions were as follows:

- **Damage initiation criterion:** The different strain-based initiation damage criteria (MAXE, QUADE and MAXPE) showed that, notwithstanding the type of adhesive, all criteria provided large errors. The stress-based MAXPS criterion also attained large P_m deviations. Oppositely, the QUADS and MAXS stress-based criteria presented better accuracy for the adhesives Araldite® AV138 and Araldite® 2015 with the QUADS criterion (average deviations of 5.9% for the Araldite® AV138 and 3.8% for the adhesive Araldite® 2015). The Sikaforce® 7752 results were not satisfactory, yet the MAXS criterion presented the closer predictions.
- **Damage growth criterion:** For the adhesive Araldite® AV38, P_m results showed that the best criterion was the BK with $\eta=2.5$ (average error of 4.1%) despite, for the limit L_O values, P_m had been wrongly estimated by $\approx 7.3\%$. P_m for the moderate ductile adhesive Araldite® 2015 was best predicted by a Power law criterion with $\alpha=1$ (average error of 3.79%), yet it also presented an average P_m deviation of 6.8% for the two limit L_O values. Regarding the strength prediction of the ductile adhesive Sikaforce® 7752, none of the tested criteria was able to accurately evaluate it. P_m was under predicted by an average of $\approx 13\%$ for all simulations performed.

Former studies addressed the effect of the CZM law shape [8] and cohesive parameters [13] on the strength prediction of SLJ which, together with the present analysis, constitute an integrated analysis of this modelling technique applied to bonded joints. Upon the conclusions of these works, it becomes easier to choose the best set of numerical conditions for an accurate P_m prediction.

References

- [1] E.W. Petrie, Handbook of adhesives and sealants, 2nd ed ed., McGraw-Hill, New York, 1999.
- [2] O. Volkersen, Die Niekraftverteilung in zugbeanspruchten mit konstanten laschenquerschnitten, Luftfahrtforschung 15 (1938) 41-47.
- [3] G.I. Barenblatt, The formation of equilibrium cracks during brittle fracture. General ideas and hypotheses. Axially-symmetric cracks, Journal of Applied Mathematics and Mechanics 23(3) (1959) 622-636.
- [4] D.S. Dugdale, Yielding of steel sheets containing slits, J. Mech. Phys. Solids 8(2) (1960) 100-104.
- [5] P. Feraren, H.M. Jensen, Cohesive zone modelling of interface fracture near flaws in adhesive joints, Eng. Fract. Mech. 71(15) (2004) 2125-2142.
- [6] P.A. Gustafson, A.M. Waas, The influence of adhesive constitutive parameters in cohesive zone finite element models of adhesively bonded joints, Int. J. Solids. Struct. 46(10) (2009) 2201-2215.
- [7] R.D.S.G. Campilho, M.D. Banea, A.M.G. Pinto, L.F.M. da Silva, A.M.P. de Jesus, Strength prediction of single- and double-lap joints by standard and extended finite element modelling, Int. J. Adhes. Adhes. 31(5) (2011) 363-372.
- [8] R.D.S.G. Campilho, M.D. Banea, J.A.B.P. Neto, L.F.M. da Silva, Modelling adhesive joints with cohesive zone models: effect of the cohesive law shape of the adhesive layer, Int. J. Adhes. Adhes. 44 (2013) 48-56.
- [9] T.M.S. Faneco, R.D.S.G. Campilho, F.J.G. da Silva, R.M. Lopes, Strength and fracture characterization of a novel polyurethane adhesive for the automotive industry, J. Test. Eval. (2016) DOI: 10.1520/JTE20150335.
- [10] ABAQUS® Documentation, Dassault Systèmes, Vélizy-Villacoublay, 2009.
- [11] J. Jing, F. Gao, J. Johnson, F.Z. Liang, R.L. Williams, J. Qu, Simulation of dynamic fracture along solder-pad interfaces using a cohesive zone model, Eng. Fail. Anal. 16(5) (2009) 1579-1586.
- [12] M.L. Benzeggagh, M. Kenane, Measurement of mixed-mode delamination fracture toughness of unidirectional glass/epoxy composites with mixed-mode bending apparatus, Composites Science and Technology 56(4) (1996) 439-449.
- [13] R.D.S.G. Campilho, M.D. Banea, J.A.B.P. Neto, L.F.M. da Silva, Modelling of single-lap joints using cohesive zone models: Effect of the cohesive parameters on the output of the simulations, J. Adhesion 88(4-6) (2012) 513-533.